



## Smart Packaging from Durian Seed Starch for Real-Time Quality Classification using DenseNet-121

<sup>1</sup>Putri Nutriastuti



Graduate School of Science Education, University of Bengkulu, Bengkulu, 38371, Indonesia

<sup>2</sup>Euis Nursaadah



Graduate School of Science Education, University of Bengkulu, Bengkulu, 38371, Indonesia

<sup>3</sup>Azvadennys Vasiguhamiaz



Perseverance Technology Co., Ltd., New Taipei City, 243303, Taiwan

<sup>4</sup>Aceng Ruyani



Graduate School of Science Education, University of Bengkulu, Bengkulu, 38371, Indonesia

<sup>5</sup>Nurhamidah



Graduate School of Science Education, University of Bengkulu, Bengkulu, 38371, Indonesia

<sup>6</sup>M. Lutfi Firdaus



Graduate School of Science Education, University of Bengkulu, Bengkulu, 38371, Indonesia

---

### Article Info

#### Article history:

Accepted 22 April 2026

---

#### Keywords:

DenseNet121;  
Digital Image Analysis;  
Edible film;  
Food safety;  
Smart packaging.

---

### ABSTRACT

This study used smart packaging made from durian seed starch with butterfly pea flower extract and applied the DenseNet121 deep learning model for real-time quality classification. Colorimetric analysis revealed a significant transition from Hue  $\sim 92^\circ$  to Hue  $\sim 289^\circ$  as food quality deteriorated due to pH changes. This study aimed to introduce a non-destructive vision-based classification framework utilizing the DenseNet121 deep learning architecture to demonstrate its effectiveness as a real time food freshness monitor. The dataset was divided into 70% training set, 20% validation set, and 10% test set to ensure robust model development. Performance was evaluated using accuracy, precision, recall, and F1 score. This methodology integrated physicochemical (pH) analysis with the development of a DenseNet121 architecture based Deep Learning model to classify food freshness phases. The results showed that edible films derived from durian seed starch and butterfly pea flower extract were capable of being indicators of food freshness. The dataset consisted of 160 images captured during a 12day experiment, which was expanded using stochastic data augmentation to improve model generalization. Computationally, the model achieved convergence with a training accuracy of 96% with loss 0.14 and achieved an internal testing accuracy of 0.94. Although testing on an external dataset recorded an accuracy of 0.78 due to environmental variability. This study proposes the first integration of durian seed starch based smart packaging with DenseNet121 architecture for automatic freshness classification of lempuk durian, providing a new approach for continuous food quality monitoring. These findings provide a quantitative basis for the application of applied mathematics and computer vision in sustainable food logistics.

*This is an open access article under the [CC BY-SA](https://creativecommons.org/licenses/by-sa/4.0/) license.*



**Corresponding Author:**

Euis Nursaadah  
 Graduate School of Science Education,  
 University of Bengkulu  
 Email: [euis@umib.ac.id](mailto:euis@umib.ac.id)

**1. INTRODUCTION**

Classification of lempuk durian freshness is modeled as a functional mapping  $f$  which transforms high-dimensional input tensors into a discrete label space.

This research uses the DenseNet121 model, where each layer  $l$  receives input as a concatenation of features from all previous layers  $x_1 = ([x_0, \dots, x_{l-1}])$  [1]. This mathematical formulation mitigates the vanishing gradient problem and improves the propagation of low-level chromatic features, enabling high fidelity classification even on limited image datasets. The development of colorimetric sensors from durian seed starch shows promising potential, despite the lack of a standard framework to bridge the gap between organic color changes and digital input models. This results in the potential loss of information during the feature extraction process. To address this structured problem, the study was guided by 3 research questions, namely: how can colorimetric sensor data from durian seed starch be formally represented in digital color space to optimize feature extraction for deep learning models? what extent can the DenseNet121 architecture maintain classification stability during real time pH monitoring amid dynamic color changes  $\Delta E$  ?.

Therefore, this study aims to formalize the representation of colorimetric sensor data as high dimensional tensor input ( $X \in R^{N \times I \times J \times K}$ ) [2].  $N$  shows the number of samples.  $I \times J$  presenting spatial resolution, and  $K = 3$  is an RGB color channel. The classification task is defined  $f: x \rightarrow y$ .

$y \in \{c_1, c_2, \dots, c_8\}$  is a set of categorical freshness states (V1-V4). The DenseNet121 architecture acts as a function  $f$ , which utilizes dense connectivity to extract chromatic features  $\phi(x)$  through non-linear transformations. Food freshness classification from image-based sensors can be formulated as a functional mapping problem. This study uses the DenseNet-121 architecture, which has been proven mathematically efficient in feature propagation and parameter optimization through its dense connectivity [3]. Representing input sensor data as a fourth order tensor, utilize deep neural operators to minimize the difference between predicted and actual freshness states using categorical cross-entropy optimization.

Machine processing systems can collect parameters such as geometric shape, texture, and pixel details invisible to the human eye to non destructively monitor food processing and safety [4]. This research builds a quantitative framework for the application of computer vision and applied mathematics in sustainable food logistics.

**2. RESEARCH METHOD**

This study implements a fine tuned DenseNet121 architecture with a dense feature reuse mechanism to classify colorimetric sensor images into eight food freshness states, which are validated through optimization of the Categorical Cross Entropy loss function on the Python TensorFlow computing environment with tensor input resolution be seen in equation (11)(12).

The model was trained with a multi class framework consisting of 8 categories (V1-V4 Fresh and V1-V4 Spoiled). In practical applications, the categories are combined into a binary classification (Fresh vs. Spoiled) to provide a clear freshness indicator for users, be seen in equation (13).

The model was implemented using Python 3.9 and the TensorFlow 2.20.0 framework. Training was performed on a CPU: Intel Core i9-14900K GPU: RTX 4060 TWIN EDGE OC 8GB RAM: TEAM Delta DDR5 32GB 6000Mhz with a fixed learning rate of  $10^{-4}$  and a batch size of 32.

The study used the Adam optimizer to minimize the categorical cross-entropy loss. All convolutional layers of the pre-trained DenseNet-121 were frozen to prevent overfitting. This strategy ensures that the model maintains strong low-level feature extraction capabilities while optimizing the final classification layer for specific pH indicator patterns.

**2.1. Research Design**

This study used an integrated research design that combines laboratory experimental and computational methods (Figure 1). An experimental approach was used to synthesize smart edible films from durian seed starch and butterfly pea flower extract, while a computational approach was applied to develop a nondestructive detection system. This mixed methods design was chosen because it allows correlation between the physical properties of the material and digital visual data, thus converting qualitative color changes into quantitative physical and chemical information.

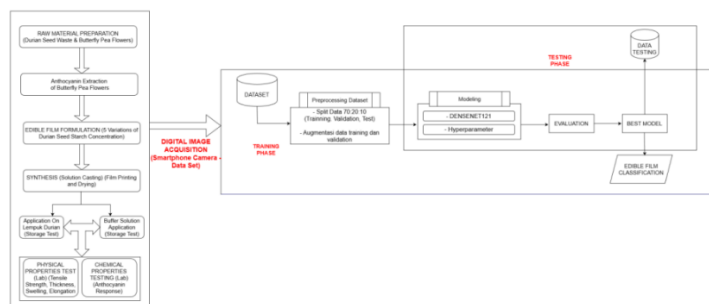


Figure 1. Research Flow Diagram

Based on the Figure 1, the study, which combines food innovation with deep learning technology, involves mixing durian seed waste and butterfly pea flower extract into an edible film [5], [6]. The integration of DenseNet121 enables automatic and consistent image feature extraction, reducing the subjectivity common in sensory testing and avoiding the destructive nature of traditional pH meter measurements. Digital film images captured using a smartphone were digitized and modeled to build the dataset, the data is then processed using the DenseNet121 architecture through a rigorous training and evaluation phase [7]. To improve transparency and reproducibility, the computational process is described in detail, including the image pre-processing stage, the splitting of training and testing data, and the model training with hyperparameter optimization such as learning rate, batch size and number of epochs.

Color change analysis is a visual indicator that has been widely used to trigger the film's response to pH changes, in line with the informative role of smart packaging [8]. The use of a representative food model (lempuk durian) and a controlled buffer solution system was chosen to maintain methodological focus and minimize confounding variables, allowing for a more valid and in-depth analysis of the relationship between pH changes, material response, and classification model performance.

The end result is an intelligent model capable of automatically and accurately classifying edible film quality. This integration aims to create a practical and cost-effective non destructive quality control tool.

## 2.2. Data Source and Variables

The primary data source in this study was 4,200 digital images acquired using a smartphone camera from edible film samples. Lighting variations were applied through data augmentation in the form of brightness and contrast adjustments during model training, allowing DenseNet121 to consistently extract color features even when the images were captured in darker or brighter conditions.

Image capture was performed under controlled conditions using a closed imaging box to minimize the influence of ambient light. The lighting source used a 10-watt white LED lamp positioned at a distance of  $\pm 10$  cm from the edible film surface, with the smartphone camera positioned fixed and perpendicular to the sample. All images were captured without using a flash with consistent camera settings to ensure uniform image quality. To ensure consistency, all images underwent preprocessing. This technique effectively reduces the model's dependence on absolute lighting intensity and focuses the learning process on the edible film intrinsic chromatic characteristics.

This image data serves as the main input for the DenseNet121 Deep Learning model to recognize the characteristics of visual materials [7]. The dataset consists of digital images capturing the chromatic response of smart biodegradable films used as active packaging for lempuk durian samples during storage period. To address labeling concerns, this study defines eight distinct classes derived from the interaction between four film formulations and two critical freshness states. Labeling criteria for Day 0 (Fresh) and Day 12 (Rotten) were established based on the critical chromatic transition threshold of an anthocyanin based smart indicator and the onset of mold. Quantitatively, this transition is validated by a significant shift in the hue angle ( $h^\circ$ ), moving from the yellow green region ( $\approx 92^\circ$ ) in the initial state to the purple-blue region ( $\approx 289^\circ$ ) as the quality deteriorates [9]. This transformation reflects the chemical kinetics of anthocyanin extract in response to pH changes in the packaging, primarily driven by the accumulation of organic acids during the degradation of the [10]. These findings are consistent with [11], which reported that the shelf-life stability of durian-based products typically reaches a critical limit between Days 10 and 12. In the absence of direct microbial quantification, this study used chronological storage and objective colorimetric shifts to serve as indicators of spoilage. We acknowledge this as a limitation therefore, the generalizability of the model is specifically tailored to detect pH-induced chromatic kinetics, and its real-world application should be interpreted in the context of this chemical visual marker.

This transition serves as a representation of the chemical breakdown of lempuk durian, thereby changing the pH of the film environment. Each image is formalized as an input tensor ( $X \in R^{4200 \times 150 \times 150 \times 3}$ ) mapping these specific chromatic variables into a high dimensional feature space for automated classification.

### 2.3. Data Collection Procedure

The data collection procedure was carried out through a hybrid experimental approach that integrates physical material testing with systematic digital data acquisition. The process begins with the synthesis of edible films using a solution molding method with a dehydrator at 55 °C for 150 minutes, which is then followed by physical and chemical characterization at two different locations.

Applied directly to lempuk durian, storage conditions were modified to accelerate dynamic changes in the material's quality. This study created a humid microenvironment by inserting wet cotton into the storage container. This increased humidity effectively triggered changes in the lempuk durian and edible film more rapidly. Edible films were stored under laboratory conditions at an ambient temperature of 30 °C. These conditions were chosen to simulate the standard storage environment for lempuk durian.

While accelerated degradation protocols provide a controlled framework for kinetic observations, the lack of microbiological validation may limit the generalizability of findings to real world storage conditions.

The model detected visual indicators of edible film degradation on day 12, determined through macroscopic observation, which showed the appearance of mycelium and spore pigmentation on the sample surface. These visual characteristics, according to [12] definitive signs of damage by fungi that distinguish it from purely chemical degradation. Consequently, models should be viewed as reliable indicators within predetermined experimental parameters. The use of colorimetric parameters and the appearance of visual mycelium was chosen because these parameters can represent the threshold of consumer acceptance of food freshness. Future research should integrate microbiological quantification to further calibrate model sensitivity to diverse microbial populations in uncontrolled environments.

During the 12-day observation period, visual changes and food quality degradation were periodically documented to capture each phase transition of the material. A total of 4.200 digital images were collected, maintaining standardized focal lengths and light intensities to minimize bias in the data set. This approach to accelerating reactions through humidity modification allowed the researchers to obtain a broad spectrum of data, ranging from "Fresh" to "Spoiled" conditions, which were then used as the basis for training the DenseNet121 deep learning architecture. The details of the edible film variations are adapted from several previous studies [13], [14], [15] the mixture is as follows:

**Table 1.** Edible Film Mix Variations (Recipe Edible Film)

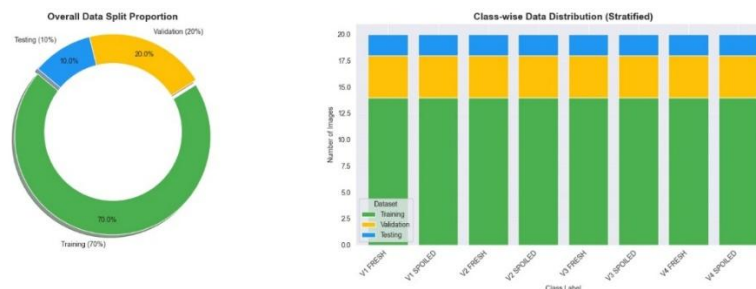
Variation	Durian Seed Flour	Cassava flour	Water	Gelatin	Glycerol	Butterfly Pea Extract
V1	1.8 g	12 g	70 %	2 g	3 mL	3 mL
V2	3.6 g	10.2 g	70 %	2 g	3 mL	3 mL
V3	7.2 g	6.6 g	70 %	2 g	3 mL	3 mL
V4	10.8 g	3 g	70 %	2 g	3 mL	3 mL

### 2.4. Analytical Methods or Algorithms

These four mechanical parameters are important indicators in determining the durability of the durian seed starch matrix during the storage period of lempuk durian.

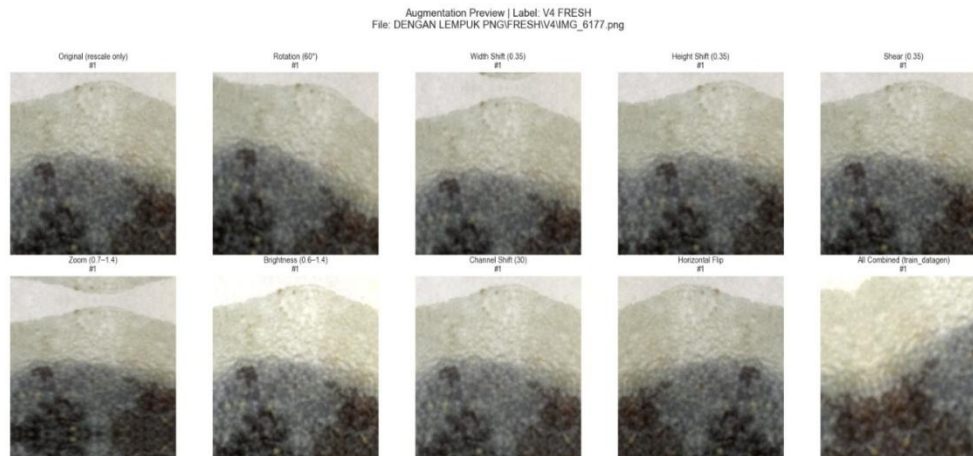
This computational framework focuses on utilizing deep learning convolutional neural network (CNN) heterogeneous visual characteristics of edible films, such as color lines, surface textures, and structural defects to predict film properties and freshness of lempuk durian with the following steps [16], [17]:

- Dataset Preparation:** To ensure the objectivity of the model, Undersampling technique was used to balance the amount of image data in the "Fresh" and "Spoiled" categories across the four edible film variations.
- Data Division:** The dataset is divided systematically in the dataset pre-processing, namely 70% for training, 20% for validation, and 10% for testing.



**Figure 2.** Data Division

- c. **Image Augmentation:** To improve the model's generalization capabilities, the training data underwent extensive augmentation, including pixel normalization, rotation up to  $30^\circ$ , horizontal/vertical shift, shear, zoom, and horizontal image flip. Augmentation parameters include high-degree rotation ( $60^\circ$ ), aggressive spatial shift (0.35), and wide brightness fluctuations (0.6 - 1.4). The transformations ensure that the DenseNet-121 architecture prioritizes the intrinsic chromatic transitions of the anthocyanin-based indicators over extrinsic noise, such as lighting inconsistencies and varying camera perspectives.



**Figure 3.** Augmentation Effect on Label V4 Fresh

- d. **Modeling:** The edible film classification system uses DenseNet121. The DenseNet121 architecture was implemented as the baseline model for transfer learning in the edible film classification task. In this study, all layers in the base model were frozen to retain the features learned from the ImageNet dataset. This decision was made due to the limited size of the research dataset, and using all parameters for re-fitting risks overfitting. Initial testing using fine-tuning methods resulted in significant divergence between training and validation accuracy. Therefore, the frozen configuration was chosen to maintain model stability and ensure better generalization on the test data. This model was implemented by setting the input size to  $150 \times 150$ , according to the specifications in Table 3. All layers in the baseline model were set as non trainable to retain the features learned from the ImageNet dataset. On top of the baseline model, Global Average Pooling and Batch Normalization layers were added to efficiently process features. Next, a fully-connected layer was built consisting of one Dense layer with 256 neurons using ReLU activation, and a Dropout (0.4) layer to prevent overfitting. The final layer used a Softmax activation function with 8 neurons, adjusted to the number of target classification classes. The model was drilled using the Adam optimizer and the Categorical Cross Entropy loss function. After 37 the model got its best results with accuracy 96% and loss 0.14 because it implemented 3 callbacks (Best Weights, Early Stopping, Reduce LR) so the model knows its best limits. Additionally, the Adam optimizer trains on the data, allowing several parameters to be adjusted during the model training process. After training, the model with the highest accuracy is selected for use in classifying edible films. Details of the modeling steps are shown in Table 3.

**Table 2.** Model Hyper parameters

Hyperparameter	Value
Pre-trained	DenseNet121
Input Shape	$150 \times 150$
Layer	Global Average Pooling, Batch Normalization
Dense, Activation	256, ReLU
Dropout	0,4
Dense, Activation	8, Softmax
Optimizer	Adam
Loss function	Categorical Cross Entropy
Epoch	100

- e. **Training Optimization**

The training process is managed using model checkpoint to store optimal weights, early stopping to prevent overfitting, and reduce  $\theta_0$  (LR) to stabilize convergence when plateaus occur. The color change in smart food packaging during storage, in color analysis this is called the total color difference  $\Delta E$ .

- f. Three color coordinates of the film were determined under controlled conditions, including  $L$  = lightness,  $a$  = greenness-redness, and  $b$  = blueness-yellowness. The total color difference ( $\Delta E$ ) was calculated using the following formula [9], [18].

$$\Delta E = \sqrt{(L^* - L)^2 + (a^* - a)^2 + (b^* - b)^2} \quad (4)$$

- g. Classifier Performance Metrics

Accuracy is the number of correct prediction proposals. The formula for calculating accuracy can be seen in equation (5).

$$Accuracy = \frac{TP + TN}{TP + TN + FP + FN} \quad (5)$$

Precision is a suggestion for the number of relevant text documents controlled among all text documents selected by the system. The precision formula can be seen in equation (6).

$$Precision = \frac{TP}{TP + FP} \quad (6)$$

Recall is the proportion of the number of controlled relevant text documents, indicating how many positive cases were correctly detected by the model. The recall formula can be expressed as (7).

$$Recall = \frac{TP}{TP + FN} \quad (7)$$

False Positive Rate (FPR) is used to measure how often a model incorrectly classifies negative data as positive. The FPR formula can be seen in equation (8).

$$FPR = \frac{FP}{FP + TN} \quad (8)$$

F1 score. This metric is the most widely used member of the parametric F-measure family, used to assess classification performance. The F1 score is defined as the harmonic mean of precision and recall and has the following form:

$$F1 = 2 \frac{Precision \cdot Recall}{Precision + Recall} \quad (9)$$

AUC is used to measure the model's ability to differentiate (discriminate) between positive and negative classes as a whole, without relying on a specific threshold value. The recall formula can be expressed as (10).

$$AUC = \sum_{i=1}^{n-1} (FPR_{i+1} - FPR_i) \frac{TPR_i + TPR_{i+1}}{2} \quad (10)$$

To optimize the parameters of the DenseNet121 model ( $\theta$ ), this study uses the Categorical Cross-Entropy (CCE) loss function. This function measures the discrepancy between the probability distribution predicted by the model and the actual labels (ground truth). Mathematically, CCE is defined as follows:

$$\mathcal{L}(\theta) = - \sum_{i=1}^c y_i \log(\hat{y}_i) \quad (11)$$

The input images are mathematically represented as a fourth-order tensor, This tensor representation allows the DenseNet-121 architecture to perform high-dimensional feature extraction through convolutional operators.

$$(X \in R^{N \times I \times J \times K}) \quad (12)$$

Classification Framework and Class Definition, through a functional aggregation, where:

$$Y = \begin{cases} 1(Fresh), & f \hat{y} \in (c_1, c_2, c_3, c_4) \\ 0(Spoiled), & f \hat{y} \in (c_1, c_2, c_3, c_4) \end{cases} \quad (13)$$

The classification performance of the DenseNet121 model was evaluated using a confusion matrix to binarobtain key performance indicators. In this study, True Positives (TP) represent samples correctly classified as 'Spoiled' (degraded), while True Negatives (TN) indicate samples accurately identified as 'Fresh'. Conversely, False Positives (FP) refer to 'Fresh' samples incorrectly labeled as 'Spoiled', and False

Negatives (FN) indicate 'Spoiled' samples incorrectly classified as 'Fresh'. Based on the experimental results shown in Figure 6, the model achieved a perfect diagonal distribution with zero values for FP and FN, resulting in non-absolute accuracy, F1 score, and ROC-AUC of less than 1.0. These results demonstrate potential applications in differentiating food quality across all types of plastic food packaging.

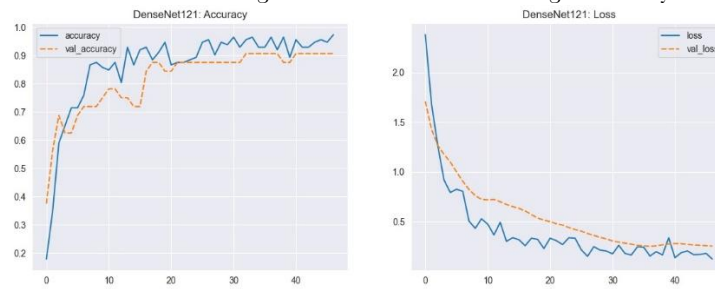
**2.5. Analytical Methods or Algorithms**

The implementation of this research was supported by a combination of standard physical instruments and computational software. Digital image acquisition was performed using a high-resolution smartphone camera as the primary sensor to capture visual changes in the samples. For the computational phase, the system was developed using the Python programming language. Deep learning libraries, including TensorFlow, were used for model construction and training. Image processing and augmentation were performed using OpenCV and Pillow, while data visualization and statistical evaluation (Classification Report, Confusion Matrix, and training graphs) were executed using Matplotlib and Scikit-learn.

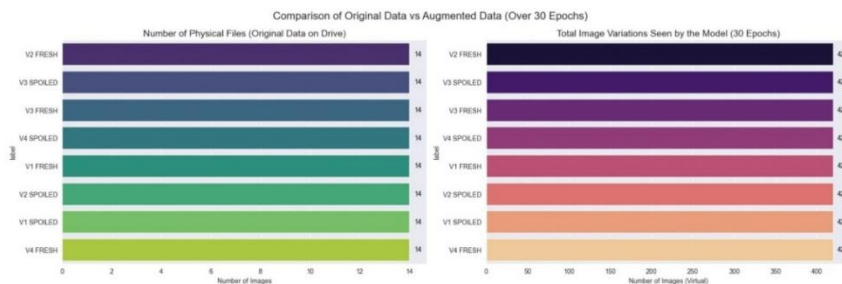
**3. RESULT AND ANALYSIS**

**3.1. Densenet121 Model**

Table 3 shows the implementation of the pre-trained architecture with a good hyperparameter configuration, including the Adam optimizer and the Categorical Cross Entropy loss function. The applied training strategy involves the use of Global Average Pooling and Batch Normalization layers, which have proven very effective in extracting important features from 150 x 150 pixel inputs. Figure 6 shows that significant performance improvements occur in the early epochs and reach convergence before the 30th epoch. The training and validation accuracy values are close to 96% with very small loss value of 0.14. The use of a Dense layer with 256 neurons and a Dropout 0.4 regularization technique significantly contributes to the model's ability to achieve high stability and prevent the risk of overfitting. DenseNet121 achieves high accuracy on small datasets [19].



**Figure 4.** Hyperparameter Table And Model Performance Graph



**Figure 5.** Performance And Configuration of the Classification Model

Applying data augmentation improves accuracy by 94% by expanding the variability of texture features in the feature space. This prevents the model from overfitting to background details (figure 7). The application of augmentation during the training process successfully increased the variety of images learned by the model to 420 virtual images per class. This representation provides a more balanced and comprehensive database for the model to recognize feature patterns from each sample.

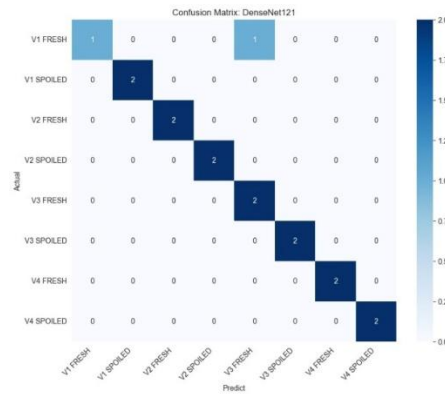


Figure 6. Confusion Matrix Model DenseNet121

All values fall along the main diagonal with no misclassification errors in Figure 8, The proposed model achieves an overall accuracy of 0.94, with an average precision and F1-score of 0.96 and 0.93, respectively. The drop in accuracy on external testing to 0.78 confirms that the model still faces challenges in generalizing features to more varied real-world conditions.

The observational variance in the V1 Fresh class recall (0.50) and V3 Fresh class precision (0.67). Consistency indicates that the model is highly effective in minimizing prediction errors [20]. The low accuracy on external data (0.78) indicates the model's sensitivity to domain shifts due to lighting variations. Final validation using a Confusion Matrix confirmed the model's excellent accuracy on the test data [21].

	precision	recall	f1-score	support
V1 FRESH	1.00	0.50	0.67	2
V1 SPOILED	1.00	1.00	1.00	2
V2 FRESH	1.00	1.00	1.00	2
V2 SPOILED	1.00	1.00	1.00	2
V3 FRESH	0.67	1.00	0.80	2
V3 SPOILED	1.00	1.00	1.00	2
V4 FRESH	1.00	1.00	1.00	2
V4 SPOILED	1.00	1.00	1.00	2
accuracy			0.94	16
macro avg	0.96	0.94	0.93	16
weighted avg	0.96	0.94	0.93	16

Figure 7. Classification report for model

Detailed analysis of individual class performance (figure 9) ROC-AUC shows that the DenseNet121 model is very robust in distinguishing degraded color features [22], which indicates that the model has a clear “feature distance” between feasible and infeasible conditions, making it more tolerant to small lighting disturbances in real-world environments. The model uses an 8 class softmax activation corresponding to 4 film formulations (V1-V4) and 2 freshness conditions fresh and spoiled. For analytical clarity in this study, the 8 classes were combined into a binary outcome fresh vs spoiled to demonstrate the model's utility in food safety monitoring. This multiclass approach is critical for capturing the subtle chromatic kinetics of the anthocyanin-based indicator. For practical implementation, these high dimensional states are mapped to a binary output can be seen in equation (13).

```

=== RESUME K-FOLD ===
Mean Accuracy      : 0.9062
Standard Deviation : 0.0797
Mean Loss         : 0.3515
Std Loss          : 0.2296
    
```

Figure 8. Resume K-Fold

Performance of DenseNet-121 94% accuracy is due to clear class separability through contrasting clusters of  $\Delta E$  values, with data augmentation strictly applied after dataset splitting to prevent overfitting. To ensure validity and strict scientific standards, 5-fold cross validation testing has been conducted and resulted in an average accuracy of 0.9062 with a standard deviation of 0.0797 (figure 10). The decrease in accuracy in external validation to 0.78 is a generalization limitation caused by environmental light interference and differences in mobile camera sensors, so color calibration steps are needed in the future to reduce the performance gap. Along with the large value of  $\Delta E$  indicates that the increase in confidence of the deep learning architecture model is effective in extracting discriminatory features from changes in color intensity to determine the quality of food products in real time and non destructively, which is in line with the findings [23].

This phenomenon confirms that the current model is still in the potential development stage and requires color normalization techniques or more extensive data augmentation to achieve robustness outside of laboratory conditions. The use of DenseNet121 is supported by literature demonstrating its superiority in handling limited datasets through deeper feature integration without redundant parameters [1]. This feature reuse characteristic allows the model to handle texture variations in greater detail than other conventional deep learning architectures [24], while ensuring the algorithm's efficiency when operating on the Android platform.

Classification intelligence resides within the DenseNet121 deep learning model and not in specific sensor hardware, the system can be deployed across a wide range of storage environments using standard mobile devices, minimizing the need for specialized infrastructure [25].

Real world implementation must overcome several critical obstacles. First, regulatory compliance regarding the migration of durian seed starch components into food matrices must be rigorously validated against food safety standards. Second, accessibility to various industrial environments, such as lighting conditions and packaging textures, remains a challenge. A strong focus on data augmentation is essential to ensure model generalizability. Finally, the cost effectiveness of this approach is supported by a waste to value model, which significantly lowers production costs compared to synthetic electrochemical sensors, making it an economically viable pathway for large scale supply chain transparency and food waste reduction [26].

### 3.2. External Validation and Generalization Analysis

To assess the models promising performance in non laboratory environments, an external validation was conducted using a disjoint dataset. The external validation yielded an overall accuracy of 0.7875, with a weighted average precision of 0.8362 and a macro-average F1-score of 0.7832, as detailed in Figure 10.

	precision	recall	f1-score	support
V1 FRESH	0.9091	1.0000	0.9524	10
V1 SPOILED	0.7692	1.0000	0.8696	10
V2 FRESH	1.0000	0.6000	0.7500	10
V2 SPOILED	0.5263	1.0000	0.6897	10
V3 FRESH	1.0000	0.7000	0.8235	10
V3 SPOILED	1.0000	0.7000	0.8235	10
V4 FRESH	0.8182	0.9000	0.8571	10
V4 SPOILED	0.6667	0.4000	0.5000	10
accuracy			0.7875	80
macro avg	0.8362	0.7875	0.7832	80
weighted avg	0.8362	0.7875	0.7832	80

Figure 9. Classification reports for external data models

The decrease in performance from 0.94 (test set) to 0.78 (external set) provides a realistic measure of the model's generalization limits. Since the proposed system relies heavily on chromatic information reflected by  $\Delta E$  values, even small illumination inconsistencies can distort color perception. Furthermore, the model exhibits sensitivity to chromatic noise under uncontrolled environmental conditions, indicating promising performance outside standard laboratory settings.

Notably, while the model maintained a perfect recall (1.0000) for V1 Fresh and V1 Spoiled, it encountered significant challenges in the V4 Spoiled category, which recorded a recall of 0.4 and an F1 score of 0.5. These results indicate that environmental variances such as fluctuating light intensities and varying camera sensor qualities affect the extraction of subtle anthocyanin color transitions in specific film formulations.




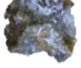











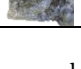
### 3.3. Computing The Color Difference

A drastic color change on day 12 from black (Hue  $\sim 90^\circ$ ) to deep blue purple (Hue  $\sim 288^\circ$ ) in table 5. The significant negative  $b^*$  value at the end of storage indicates that the anthocyanin sensor has reached its blue color saturation point, effectively masking the yellow background of the durian pulp sample.

Changes in pH during storage affect the stability of the anthocyanin structure, which functions as a color indicator in edible films. This structural transformation results in color changes measured as variations in  $\Delta E$  values. Previous studies have shown that anthocyanin-based indicators have high sensitivity to changes in pH and volatile compounds, and show a positive correlation between indicator color changes and food degradation parameters [27], [28]. This is what causes the  $\Delta E$  value in the V2 variation to reach a number above 10, which according to international standards is the limit of color change that is very easily recognized directly by the human eye [29], [30]. A higher  $\Delta E$  value indicates a clearer difference in indicator color between freshness levels, thus increasing the separation of features between classes and classification accuracy.

The  $\Delta E$  value is used as the main indicator of color changes in edible films based on butterfly pea extract, where  $\Delta E > 3$  indicates color changes that begin to be visually visible and  $\Delta E > 8$  indicates significant color changes related to a decrease in the quality of lempuk durian.

**Table 3.** Color changes of smart biodegradable film packaging as packaging for lempuk durian samples during storage

Varians	Day	L*	a*	b*	C	H	ΔE	Edible Film
V1	0 (Control)	49.720001	0.04	5.43	5.43	89,580,002	0	
	4	45.230000	-0.43	4.97	4.99	94,949,997	4.54	
	8	45.220001	-0.21	4.95	4.96	92,410,004	4.53	
	12	46.220001	0.36	-2.30	2.32	278,970,001	8.49	
V2	0 (Control)	45.450001	-0.15	3.97	3.97	92,190,002	0	
	4	39.689999	-0.50	3.12	3.16	99,080,002	5.83	
	8	39.070000	-0.47	2.97	3.00	99,070,000	6.47	
	12	41.619999	0.81	-2.36	2.49	288,950,012	7.46	
V3	0 (Control)	38.919998	-0.33	4.10	4.12	94,660,004	0	
	4	36.540001	0.05	3.87	3.87	89,260,002	2.42	
	8	36.330002	-0.96	2.67	2.84	109,860,001	3.03	
	12	50.570000	2.94	-10.48	10.88	285,679,993	18.87	
V4	0 (Control)	36.900002	-0.33	5.16	5.17	93,699,997	0	
	4	38.590000	-1.13	5.58	5.69	101,480,003	1.92	
	8	43.369999	-1.52	2.36	2.81	122,760,002	7.15	
	12	55.750000	0.14	0.91	0.92	80,970,001	19.33	

The system using DenseNet121 is capable of extracting high level chromatic spatial features, thus enabling the detection of subtle color changes invisible to the human eye or simple gas sensors at a low cost [31].

The model performance in this study has been quantitatively benchmarked against current literature. The decrease in accuracy on external data aligns with the domain shift challenge identified [32] as a major challenge in field conditions. Nevertheless, the use of DenseNet121 proved effective in recognizing early mold texture, as validated [33], but with the advantage of parameter efficiency for mobile devices. This integration of smart durian seed packaging and AI reinforces the trend of adaptive and lightweight digital food inspection systems, as developed [33].

The DenseNet-121 implementation showed a validation accuracy of 0.94, indicating the strong potential of this architecture in capturing anthocyanin chromatic transitions ( $h^\circ \approx 92^\circ \rightarrow \approx 289^\circ$ ). Smartphone based food classification can achieve high precision, although it is heavily influenced by color space and lighting [34]. While these laboratory results are promising, the model's reliability remains limited by the experimental parameters and the durian seed matrix used. Several limitations of the study need to be critically evaluated. First, the limited size of the primary dataset results in a reliance on augmentation to achieve model convergence. Second, the use of a proxy lab

eling approach based on storage days. Finally, there is a generalization gap, with accuracy dropping from 0.94 to 0.78 in external testing. This 0.16 decrease is primarily due to environmental noise and lighting variance, which are major obstacles to digital image analysis [34][35]. This model is at risk of failure under extreme lighting conditions or varying sensor calibrations. Therefore, while practical for SMBs, future widespread adoption requires the development of color normalization algorithms to mitigate the dependence on ambient light.

#### 4. CONCLUSION

This study demonstrates the potential of DenseNet-121 in classifying the freshness of lempuk durian using a smartphone-based anthocyanin indicator. training accuracy of 96% with a loss of 0.14 and a testing accuracy of 0.94. However, a performance drop to 0.78 during external testing indicates a generalization gap caused by lighting variance. Its current reliability is limited by standard illumination and a variety of laboratory trained data. Further research is needed to develop a larger, microbiologically validated dataset to improve the model's robustness before full commercial implementation. Nevertheless, these results provide an important quantitative foundation for the development of lightweight and adaptive food monitoring technologies.

## 5. REFERENCES

- [1] E. Mocsari and S. S. Stone, "Dense Net," *Cvpr*, vol. 39, no. 9, pp. 1442-1446, 2017, doi: 10.1109/CVPR.2017.243.
- [2] A. C. Chan, "From tensors to novelties: Low-dimensional representations for anomaly detection in multispectral imagery," *Machine Learning Applications*, vol. 23, p. 100858, 2026, doi: 10.1016/j.mlwa.2026.100858.
- [3] M. Shanmugavelu and M. Sannasy, "A scheme of opinion search & relevant product recommendation in social networks using stacked DenseNet121 classifier approach," *Automatika*, vol. 64, no. 2, pp. 248-258, 2023, doi: 10.1080/00051144.2022.2140389.
- [4] L. Zhu, P. Spachos, E. Pensini, and K. N. Plataniotis, "Deep learning and machine vision for food processing: A survey," *Current Research in Food Science*, vol. 4, pp. 233-249, 2021, doi: 10.1016/j.crf.2021.03.009.
- [5] C. R. Utami, W. Zuhdi, and A. N. R. Ida, "Characteristics and application of edible film from durian seed-corn starch with butterfly pea flower extract," *Asian Journal of Dairy and Food Research*, vol. 44, no. 1, pp. 1-9, 2025, doi: 10.18805/ajdf.drf-499.
- [6] C. Assyifa, Fatima, I. A. Franella, F. Halqiah, I. Sulaiman, and D. Yunita, "Application of anthocyanin extract from butterfly pea flower (*Clitoria ternatea*) as a freshness indicator," *Jurnal Teknologi Industri Pangan Unisri*, vol. 10, no. 2, pp. 137-147, 2023, doi: 10.33061/jitipari.v10i2.11078.
- [7] K. N. Rahman, S. C. Banik, R. Islam, and A. Al Fahim, "A real time monitoring system for accurate plant leaves disease detection using deep learning," *Crop Design*, vol. 4, no. 1, p. 100092, 2025, doi: 10.1016/j.cropd.2024.100092.
- [8] C. Wang *et al.*, "Preparation, characterization, and application of pH-responsive biodegradable intelligent indicator film based on rose anthocyanins," *LWT*, vol. 200, p. 116156, 2024, doi: 10.1016/j.lwt.2024.116156.
- [9] H. Ren, J. Wang, Z. Miao, F. Li, S. Yu, and P. Wu, "Multi-color composite films constructed by natural colorants and carbon dots: manipulation of color, property characterization, and application in food anti-counterfeiting packaging," *LWT*, vol. 230, p. 118243, 2025, doi: 10.1016/j.lwt.2025.118243.
- [10] F. W. Hailu, S. W. Fanta, A. A. Tsige, and M. A. Delele, "Development of simple and biodegradable pH indicator films from cellulose and anthocyanin," *Discover Sustainability*, vol. 6, no. 1, 2025, doi: 10.1007/s43621-025-00916-4.
- [11] Y. A. Septiati, M. Karmimi, A. Kamaludin, and F. Fatimah, "Analisis Luas Bukaannya Penyimpanan Makanan terhadap Kadar Air dan Total Jamur Makanan Terkemas Bioplastik," *Jurnal Kesehatan Lingkungan Indonesia*, vol. 23, no. 2, pp. 226-233, 2024, doi: 10.14710/jkli.23.2.226-233.
- [12] J. I. Pitt and A. D. Hocking, *Fungi and Food Spoilage 3rd Edition*, vol. 53, no. 9, 2009.
- [13] S. C. Wattimena and P. J. Patty, "Physical properties of durian (*Durio zibethinus* Murr) seed starch and its associated edible film," *Jurnal Sains Dasar*, vol. 14, no. 2, pp. 1-7, 2025, doi: 10.21831/jsd.v14i2.90720.
- [14] C. D. Alfarisi, Y. Fitri, and D. K. Nisa, "Pengaruh Penambahan Tepung Biji Durian pada Pembuatan Bioplastik," *Biosaintropis*, vol. 7, no. 1, pp. 44-55, 2021, doi: 10.33474/e-jbst.v7i1.385.
- [15] A. Istiani, N. A. Wardani, M. Kafiya, N. A. Hanifah, and Z. Nukhia, "Karakterisasi Edible Film dari Pektin Kulit Durian, Pati Singkong, dan Gliserol," *Eksergi*, vol. 21, no. 1, p. 17, 2023, doi: 10.31315/e.v21i1.10949.
- [16] W. K. Z. Oktoeberza *et al.*, "Multi-class skin cancer on imbalanced data," *Jurnal Nasional Pendidikan Teknik Informatika*, vol. 14, no. 2, pp. 421-431, 2025, doi: 10.23887/janapati.v14i2.85544.
- [17] A. L. Zahra, A. A. Arifiyanti, and T. L. I. Sugata, "Implementasi arsitektur CNN DenseNet-121 untuk identifikasi autoimun kulit dengan augmentasi data," *Jurnal Ilmiah Teknik Informatika Komunikasi*, vol. 5, no. 2, pp. 94-113, 2025, doi: 10.55606/juitik.v5i2.1026.
- [18] S. Niam, I. Ahmad, M. A. Rayhan, S. Mahmood, P. H. Jon, and M. M. Ahmed, "Machine learning-based optimization of alginate, guar gum, and pectin-based edible coatings for extended strawberry shelf life," *LWT*, vol. 233, p. 118548, 2025, doi: 10.1016/j.lwt.2025.118548.
- [19] T. Dhar *et al.*, "Molecular validation integrated reliable deep learning approach for early blight severity detection in tomato crops under protected cultivation environments," *Results in Engineering*, vol. 28, p. 107739, 2025, doi: 10.1016/j.rineng.2025.107739.
- [20] D. Chicco and G. Jurman, "The advantages of the Matthews correlation coefficient (MCC) over F1 score and accuracy in binary classification evaluation," *BMC Genomics*, vol. 21, no. 1, pp. 1-13, 2020, doi: 10.1186/s12864-019-6413-7.
- [21] S. K. Ray, M. A. Hossain, N. Islam, and M. A. F. M. Rashidul Hasan, "Enhanced plant health monitoring with dual head CNN for leaf classification and disease identification," *Journal of Agriculture and Food Research*, vol. 21, p. 101930, 2025, doi: 10.1016/j.jafr.2025.101930.
- [22] M. Mustapha *et al.*, "A hybrid machine learning approach for imbalanced irrigation water quality classification," *Desalination and Water Treatment*, vol. 321, 2025, doi: 10.1016/j.dwt.2024.100910.

- [23] N. Gul, K. Muzaffar, S. Z. A. Shah, A. Assad, H. A. Makroo, and B. N. Dar, "Deep learning hyperspectral imaging: a rapid and reliable alternative to conventional techniques in the testing of food quality and safety," *Quality Assurance and Safety of Crops and Foods*, vol. 16, no. 1, pp. 78-97, 2024, doi: 10.15586/qas.v16i1.1392.
- [24] N. Songara and M. K. Jain, *Design of qos and energy efficient vm consolidation framework for cloud data centers*, vol. 643. 2020. doi: 10.1007/978-981-15-3125-5\_19.
- [25] M. A. Mir, N. Zaidi, S. K. Chang, N. Abdelli, and K. Andrews, "Artificial intelligence applications in food science: a review of cutting-edge technologies," *Cogent Food and Agriculture*, vol. 12, no. 1, p., 2026, doi: 10.1080/23311932.2025.2606439.
- [26] L. Kumar, D. Ramakanth, K. Akhila, and K. K. Gaikwad, "Edible films and coatings for food packaging applications: a review," *Environmental Chemistry Letters*, vol. 20, no. 1, pp. 875-900, 2022, doi: 10.1007/s10311-021-01339-z.
- [27] S. Roy and J.-W. Rhim, "Anthocyanin food colorant and its application in pH-responsive color change indicator films," *Critical Reviews in Food Science and Nutrition*, vol. 61, no. 14, pp. 2297-2325, Jul. 2021, doi: 10.1080/10408398.2020.1776211.
- [28] C. Wang and C. Liu, "A pH-Sensitive Intelligent Packaging Film Harnessing Anthocyanin for Food Freshness Monitoring," *Food and Bioprocess Technology*, vol. 17, no. 12, pp. 5312-5323, 2024, doi: 10.1007/s11947-024-03431-y.
- [29] S. Gautam, M. Verma, and T. S. Lakhanpal, "Machine-learning driven design of bio-based active food packaging films with improved mechanical properties," *Sustainable Food Technology*, vol. 3, no. 6, pp. 1705-1722, 2025, doi: 10.1039/d5fb00198f.
- [30] K. Kalinowska, W. Wojnowski, and M. Tobiszewski, "Smartphones as tools for equitable food quality assessment," *Trends in Food Science and Technology*, vol. 111, pp. 271-279, 2021, doi: 10.1016/j.tifs.2021.02.068.
- [31] S. Perveen *et al.*, "Utilization of biomaterials to develop the biodegradable food packaging," *International Journal of Food Properties*, vol. 26, no. 1, pp. 1122-1139, 2023, doi: 10.1080/10942912.2023.2200606.
- [32] D. Sujatha, Dr. R. Sornakeerthi, and Dr. Sithishameem Fathima, "A Review of Fruit Disease Detection Using Deep Learning Models: Trends, Challenges, and Future Direction," *International Journal of Advanced Research and Interdisciplinary Scientific Endeavours*, vol. 3, no. 4, pp. 982-990, 2025, doi: 10.61359/11.2206-2554.
- [33] P. Treepong and N. Theera-Ampompunt, "Early bread mold detection through microscopic images using convolutional neural network: Early bread mold detection," *Current Research in Food Science*, vol. 7, no. August, p. 100574, 2023, doi: 10.1016/j.crf.2023.100574.
- [34] Y. Tjandra, G. Halim, J. Briano, and M. Tjahjono, "Smartphone-based digital image analysis for qualitative classification of food dyes using machine learning: effects of color space and lighting conditions," *Jurnal Kimia Pendidikan Kimia*, vol. 10, no. 2, pp. 309-322, 2025, doi: 10.20961/jkpk.v10i2.107520.
- [35] Y. Pan *et al.*, "A smartphone-based non-destructive multimodal deep learning approach using pH-sensitive pitaya peel films for real-time fish freshness detection," *Foods*, vol. 14, no. 10, p. 1805, 2025, doi: 10.3390/foods14101805.